Space Engineering 3
Assignment 2
1st May 2016

Global Navigation Satellite Systems

Lydia Drabsch
311217591
ldra3557@uni.sydney.edu.au

STUDENT PLAGIARISM: COURSE WORK - POLICY AND PROCEDURE COMPLIANCE STATEMENT

INDIVIDUAL / COLLABORATIVE WORK

I/We certify that:

(1) I/We have read and understood the *University of Sydney Student Plagiarism: Coursework Policy and Procedure*;

(2) I/We understand that failure to comply with the *Student Plagiarism: Coursework Policy and Procedure* can lead to the University commencing proceedings against me/us for potential student misconduct under Chapter 8 of the *University of Sydney By-Law 1999* (as amended);

(3) this Work is substantially my/our own, and to the extent that any part of this Work is not my/our own I/we have indicated that it is not my/our own by Acknowledging the Source of that part or those parts of the Work.

Name(s): Lydia Drabsch

Signature(s):
Lydia Drabsch

Date: 24/3/16

Contents

List of Figures

List of Tables

1. Introduction

Each mainQN.m file has a section called 'User Input' where the animations and state plots can be turned on/off. Also the timestep and the number of days to simulate are defined. The default settings are dt = 100 seconds and days = 1.

2. Tracking UAV from GPS

2.1 Introduction

The ephemeris data in keplerian orbital parameters were provided and used to simulate all of the satellites in the GPS constellation. A UAV was flown along a path while receiving range data from observable satellites in the GPS constellation. The data was used to track the location of the UAV relative to a set ground station. The ground station also tracked the UAV, and the two sets of data are compared to analyse the accuracy of the GPS.

2.2 Methodology

2.2.1 GPS Simulation

The satellites were simulated using the keplerian model. The positions in ECI, ECEF and LLH frames were calculated and stored in a 3D matrices with dimensions (position axis, time, satellite). The orbits are sorted into colours by the value of the right ascending node in the ephemeris data. Kepler's method relates the mean and eccentric anomalies (Mt and E) and solved using newtowns method.

2.2.2 UAV Tracking

A minimum of four satellites are required to be observed in order to solve for the 3D position of the UAV. The fourth satellite is necessary in order to account for clock bias. Clock bias is the error in the clock on the UAV, resulting in errors of the time that the signal was received. The signal carries information of when it was sent which is then transformed into distance. For more than four satellites, the system is overdetermined and must be solved approximately. The non-linear least squares (NLLS) formulation was implemented from the pseudorange measurements from the GPS.

NLLS is applied in this context by using the residual errors $\Delta\rho_0$ between the measured pseudorange and the calculated pseudorange from a system model. The residual error is minimised by iteratively updating the estimate of the states $X_0 = [x_0, y_0, z_0, cb_0]^T$. The minimisation algorithm is characterised by the cost function $J = \frac{1}{2}\Delta\rho_0^T W \Delta\rho_0$ with a diagonal weighting matrix W which contains the measurement confidence and coupling errors. The state is progressed forward by the jacobian H of the system model and reevaluated about each stationary point due to the non-linearity of the system. The state X is updated $X = X_0 + \Delta X$ by the least squares optimisation $\Delta X = (H^T W H)^{-1} H^T W \Delta\rho_0$ and. Iteration continues until convergence, when ΔX is small. The initial state for each timestep is guessed as the position calculated in the previous timestep. The location of the ground station is used as the initial guess for the first timestep.

The NLLS algorithm was run for each step in time to solve for the position of the UAV. Dilution of precision values(DOPs) were calculate for each measurement using the diagonals of $V = (H^T H)^{-1}$. DOPs are a measurement of precision for that point in time.

2.2.3 Error Detection and Correction

The error was detected by implementing constraints on the UAVs dynamics. If the UAV instantaneously accelerated at 100 m/s^2 in any direction that point in time was identified as an error. The

velocity was calculated by the change in position over one time step, and similarly for the instantaneous acceleration.

The error correction method that was implemented consisted of linearly extrapolating missing ranges in the raw data based on the location where the error was from the previous detection method. The NLLS algorithm was run again and the error detection algorithm until no more extrapolating was done. However this did not work well because the range is not a linear relationship. Maybe with a weighting matrix on this measurement it may aid error correction, but it was not a robust method. This section of the code was not implemented in **main1C.m**, see **errorcorrection.m** for the extrapolating code.

2.3 Results/Discussion

2.3.1 GPS Simulation

The keplerian model was used for the analysis as the satellites are in MEO where the atmospheric affects are minimal. Also as the inclination of the satellites are at 55° , there is only a slight affect on the argument of perigee from the oblateness of the Earth. The entire constellation is at the same inclination, therefore all of the satellites will have the same precession and is still able to have full Earth coverage. The analysis also used the simulation close to the time the TLEs were retrieved for a period of 24 hours (2 orbit periods), hence the keplerian model provides an accurate representation of the GPS constellation.

See Figures 4.1 to 4.5 for the ECI frame, ECEF frame and ground trace of the 24 hour simulation, see Table 2.1. The mission of the GPS constellation was to provide consistent global coverage for the human population. GPS achieves that by having similar orbits with uniform altitudes eccentricities and inclinations. The geometric configuration is called a 'Walker delta' configuration with equally spaced planes and equally spaced phase shifts. This geometry results in a high number of satellites observable at the mid latitudes as satellites from different orbital planes overlap as seen by the ECEF frame Fig 4.4. At the poles there is a low density of satellites as seen by the hole in the ECEF frame Fig 4.3. As the orbit is in MEO, the footprint of each satellite is large and can still provide coverage at the poles.

The orbital period is half a sidereal day, which means that each satellite returns to the original position. This improves network constancy and the location of the ground stations can be optimised for the long term.

Table 2.1: Summary of nominal orbital parameters

Orbtial Parameter	**Nominal Value**
Semi Major Axis	26 560 km
Eccentricity	¡ 0.01
Period	11.58 hrs
Inclination	55°
Phase Shift	30°
Number of planes	6

2.3.2 UAV Tracking

The UAV tracking results in LGCV from the ground station are in Fig 4.6 and the polar track in Fig 4.7. In general, there was a good agreement between the GPS tracking and the ground station tracking, however there were a few spikes of deviation. The N-E track was highly accurate, it was the D coordinate that shows the deviations. The vertical displacements must be GPS tracking errors as it is unreasonable for the UAV to accelerate that quickly. The vertical displacements line with with a

spike in clock bias Fig 4.13. This may be due to signal noise and data corruption from satellite clock drift, atmospheric effects or multipath errors.

The geometric dilution of precision Fig 4.8 spikes when the number of satellites are low Fig 4.9. However, for some lower number of satellites there is not a spike in precision error. This is because a greater distribution of the satellites across the visible sky will result in a lower GDOP. See Fig 4.12 for the best GDOP (37) with four satellites compared to the worst GDOP (3567) in Fig 4.11. The best GDOP (2.7) for the whole flight was Fig 4.10 with 9 satellites visible.

2.3.3 Error Detection and Correction

The error detection worked well, and it correlated with spikes in the clock bias as well, Fig 4.21. See Fig 4.14 for the polar plot and Fig 4.15 for the cartesian plot of the GPS track. Dilution of precision Figures 4.16, 4.18, 4.20, 4.19. The number of satellites that were visible is contained in Fig 4.17.

3. GLONASS Orbital Determination

3.1 Introduction

The Russian GNSS is called GLONASS, a system that requires 24 satellites in three orbital planes to have full global coverage. The satellites are in nearly circular orbits at an average altitude of 19130 km, period of 11 hrs and 15 min and an inclination of 65°. Each orbital plane is separated by 120°in the ascending node and consists of eight satellites. There is currently 28 satellites in orbit with 23 operational. For the following analysis, only the operational satellites are used.

3.2 Methodology

The high

Done:

TLEs for GLONASS and simulated - 3d and ground trace
brute force characterisation of the time
optimisation of ground stations

next: simulate ground station readings?

3.2.1 Optimisation of Ground Station Locations

The ground station locations were chosen based on a brute force recursion algorithm that ensures all satellites are visible to a ground station (5°mask) at all times. A 4-D logical matrix was created with the dimensions (longitude,latitude,time,satellite) where the element was set if the satellite was visible at that point in time from that location. Only locations that are on land were considered using **landmask.m** (Chad Greene, 2014) and the altitude was estimated using **ITU_P1511.m** (Luis Emiliani, 2009). For each location the total observed time of all satellites was summed and the location with the maximum observations was chosen as a ground station. For the satellites that were observed over certain times from the new ground station, the observations were removed from all other locations in the 4-D matrix. The function was called again with the unobserved satellites and the next maximum point set as a new ground station. The function **optimise.m** continues to call itself until all the satellites are always observed by at least one ground station.

The latitude grid was divided up uniformly across the spherical surface by the function $lat = \cos^{-1}(2x - 1) - \pi/2$, where $x = [0 : dx : 1]$. If there are multiple locations with the same maximum value, the centre of the largest area is selected using **regionprops.m**.

Table 3.1: Ground stations in the order chosen by the optimisation algorithm (Latitude grid size = 100, Longitude grid size = 200, Duration = 1 day, Time step = 100 sec)

Number	Location	Latitude	Longitude	Altitude (m)	Unique Timesteps
1	Antarctica	-90°	0°	2805	7584
2	Svalbard, Norway	78°	14 °	251	7553
3	Hawaii	19°	-156°	166	2263
4	Kenya	-2°	38°	849	1585
5	Brazil	-12°	-62 °	366	589
6	China	30°	105°	352	321

The fact that GLONASS belongs to Russia and that it would be desirable to have a ground station in Russia was not considered, nor was global politics or structural feasibility of the location.

3.2.2 Model the observation of a satellite

Tried to implement three sensor model rho,az,el.

3.2.3 Calculating Orbital Parameters from Observations

herrick gibbs method to calculate the velocity vector from three position measurements

3.3 Results

3.3.1 Simulation

The period of the orbits line up so perfectly with the side real day of Earth, and the phase shift in the ascension node between orbital planes that the ground trace orbits perfectly align, see Figures in section 5. On high latitudes (north or south), GLONASS' accuracy is better than that of GPS due to the orbital position of the satellites.

3.3.2 Optimisation of Ground Station Locations

It was found that four ground stations located as in Table 3.1 Vernial equinox data `http://earthsky.org/astronomy-essentials/everything-you-need-to-know-vernal-or-spring-equinox` data all TLE `https://www.celestrak.com/NORAD/elements/glo-ops.txtbutusedtlefromSpaceTrack`

4. Appendix A: Question 1

Figure 4.1: GPS 24 hr simulation with dt = 100 in ECI frame

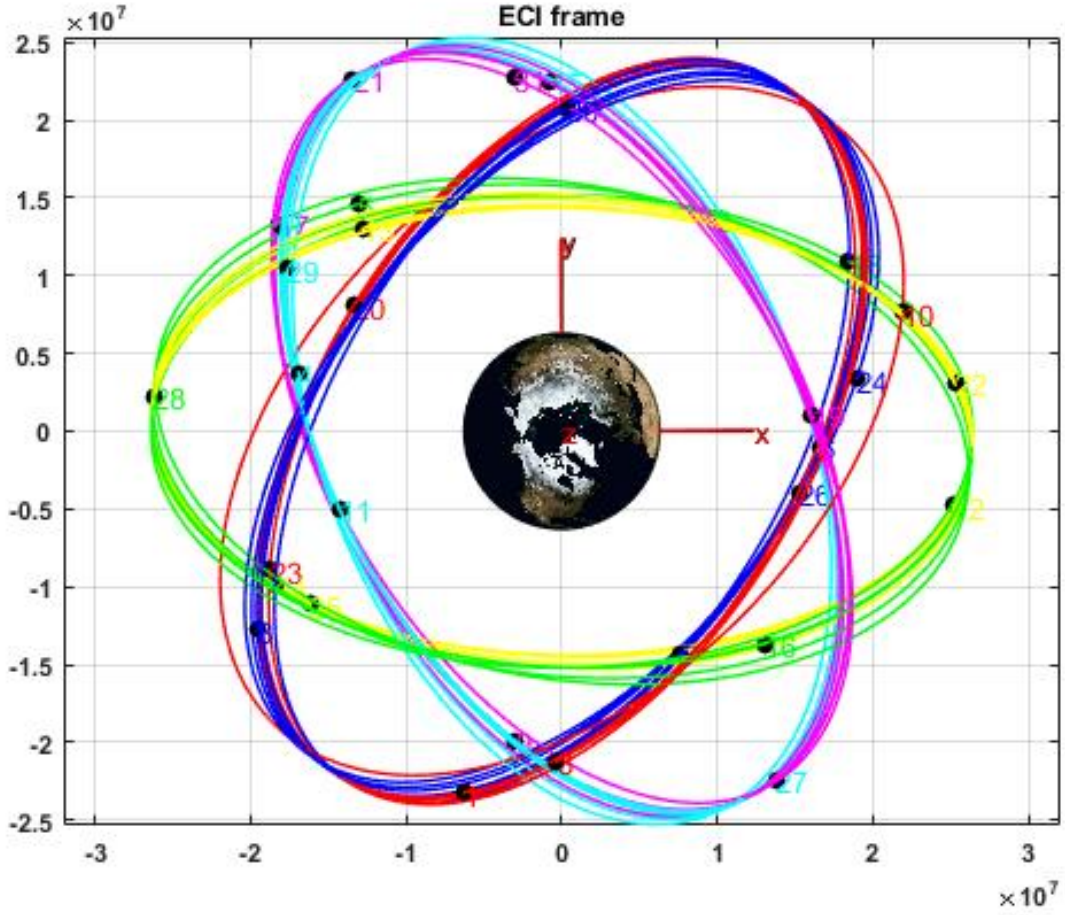

Figure 4.2: GPS 24 hr simulation with dt = 100 in ECI frame

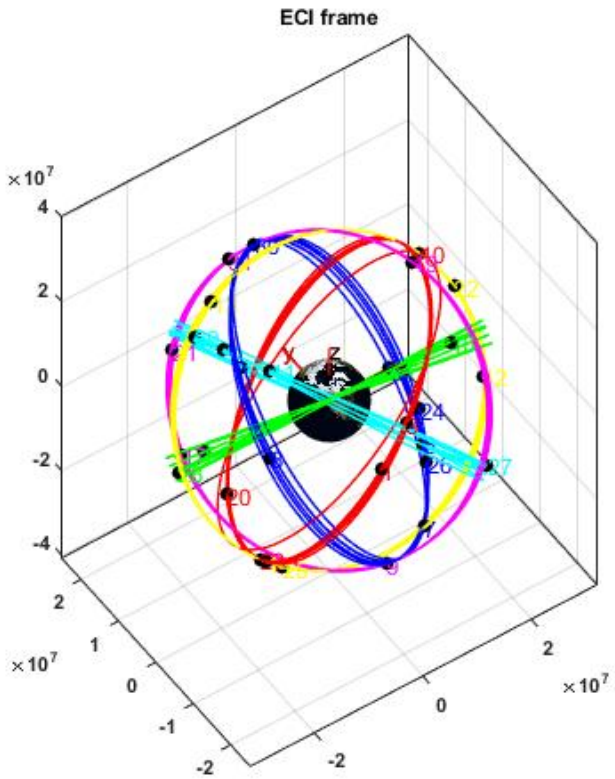

Figure 4.3: GPS 24 hr simulation with dt = 100 in ECEF frame

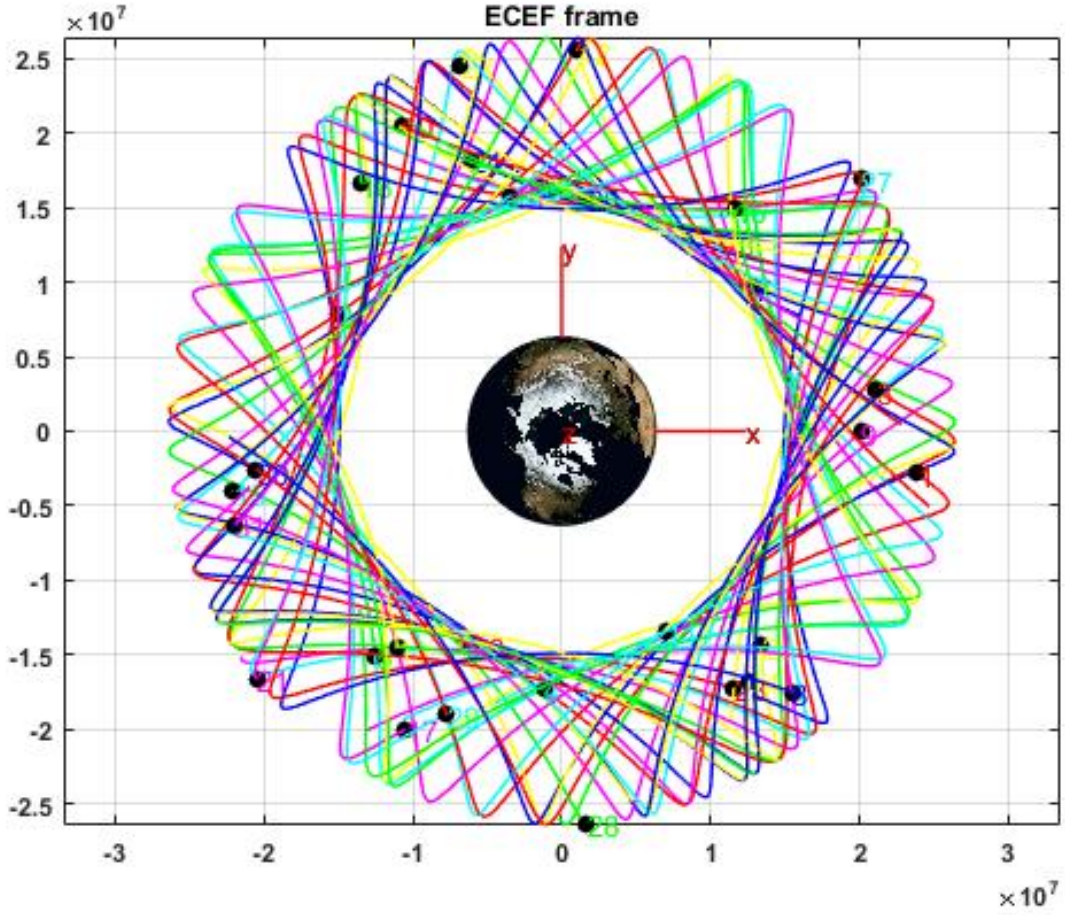

Figure 4.4: GPS 24 hr simulation with dt = 100 in ECEF frame

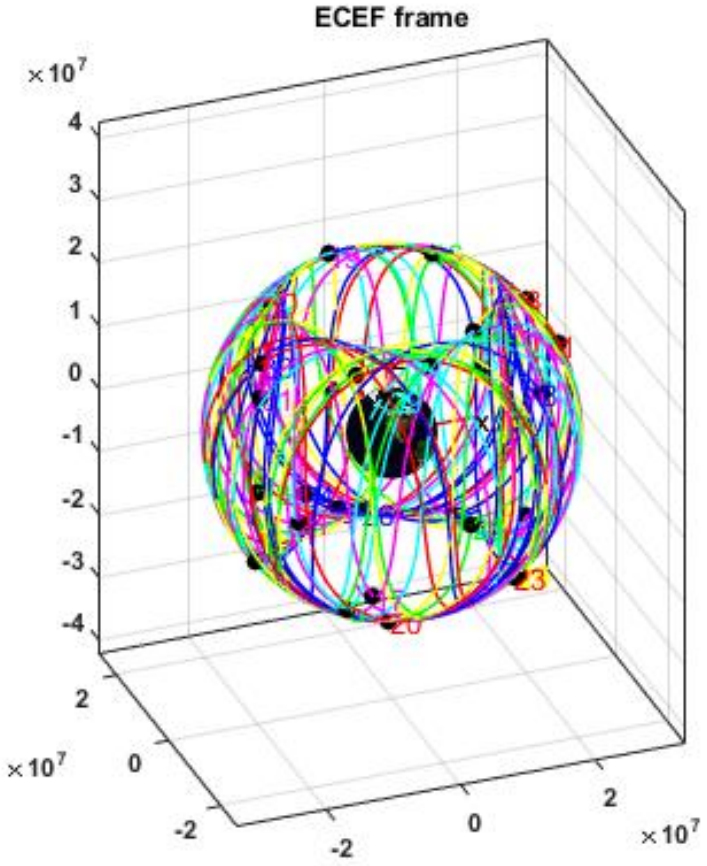

Figure 4.5: GPS 24 hr simulation with dt = 100 Ground Trace

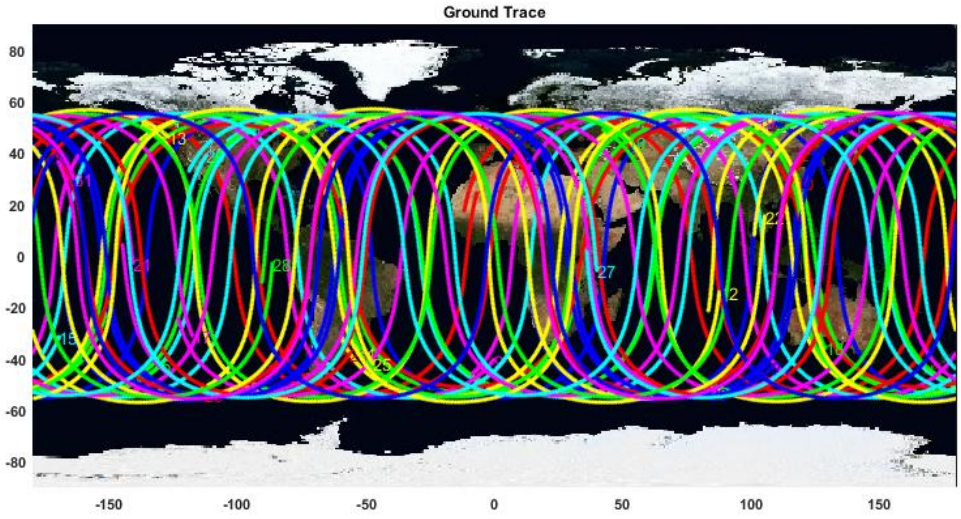

Figure 4.6: UAV Flight 1 trace in NED coordinates from the ground station at [Lat 34.76°,Long: 150.03°E, Alt: 680m]

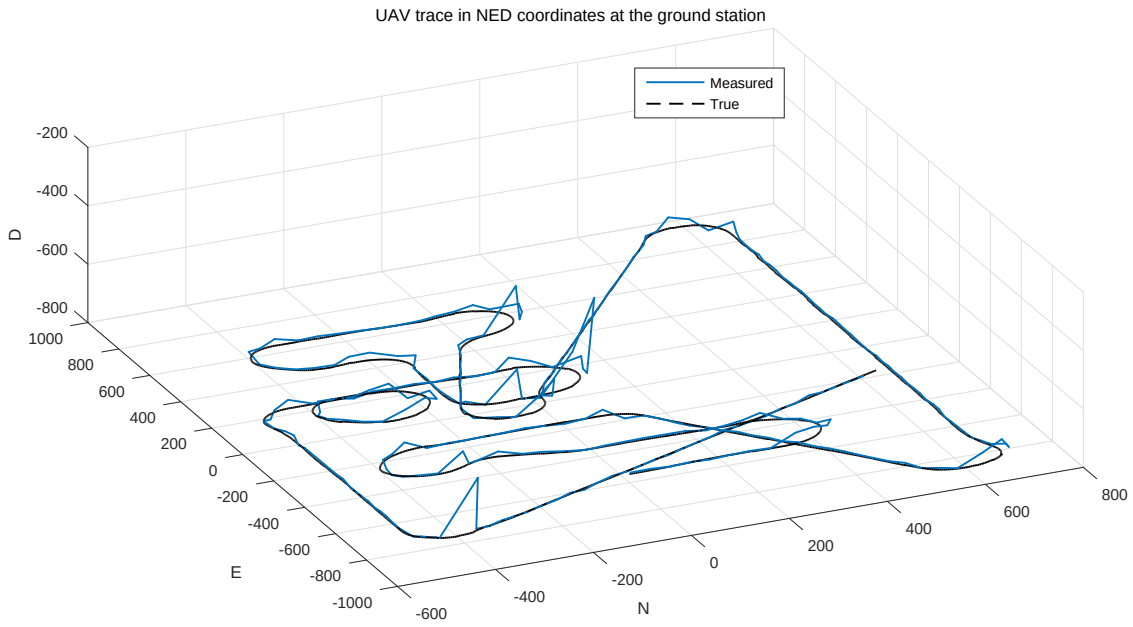

Figure 4.7: UAV Flight 1 polar trace of azimuth and elevation and location of observed satellites from ground station at [Lat 34.76°,Long: 150.03°E, Alt: 680m]

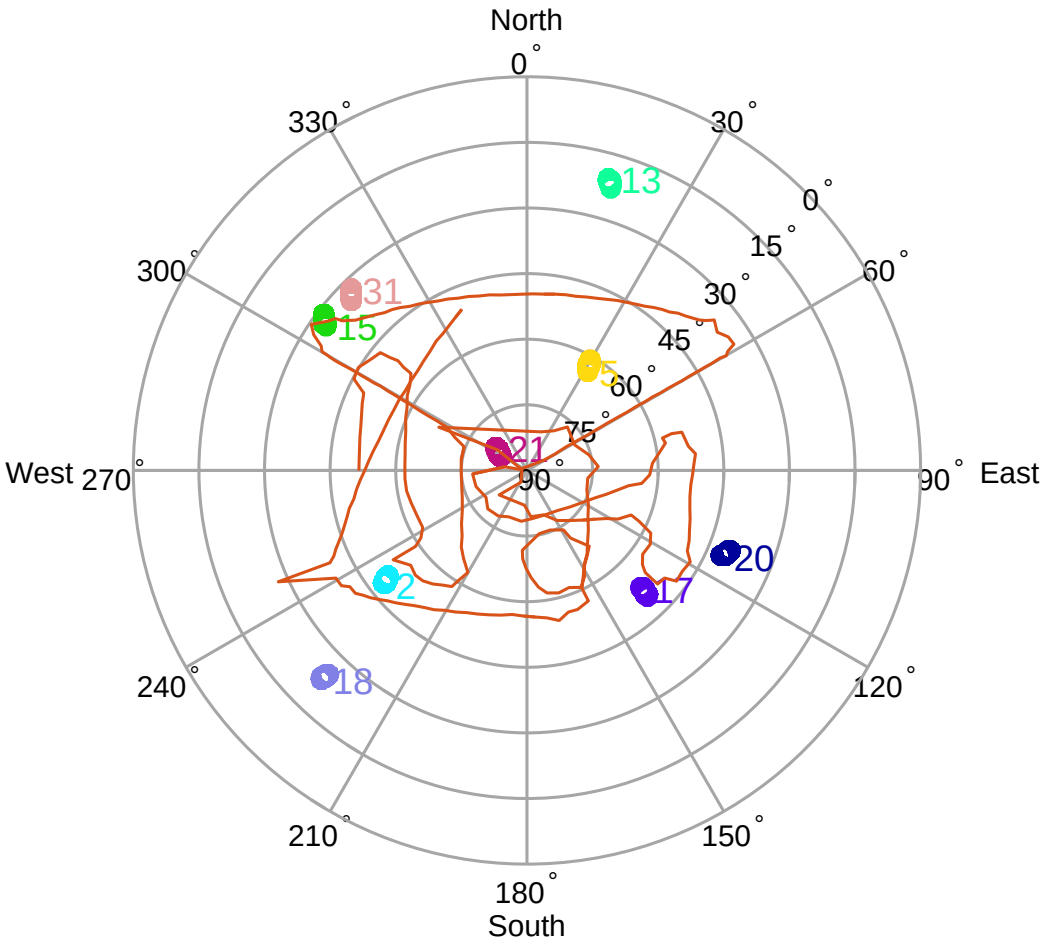

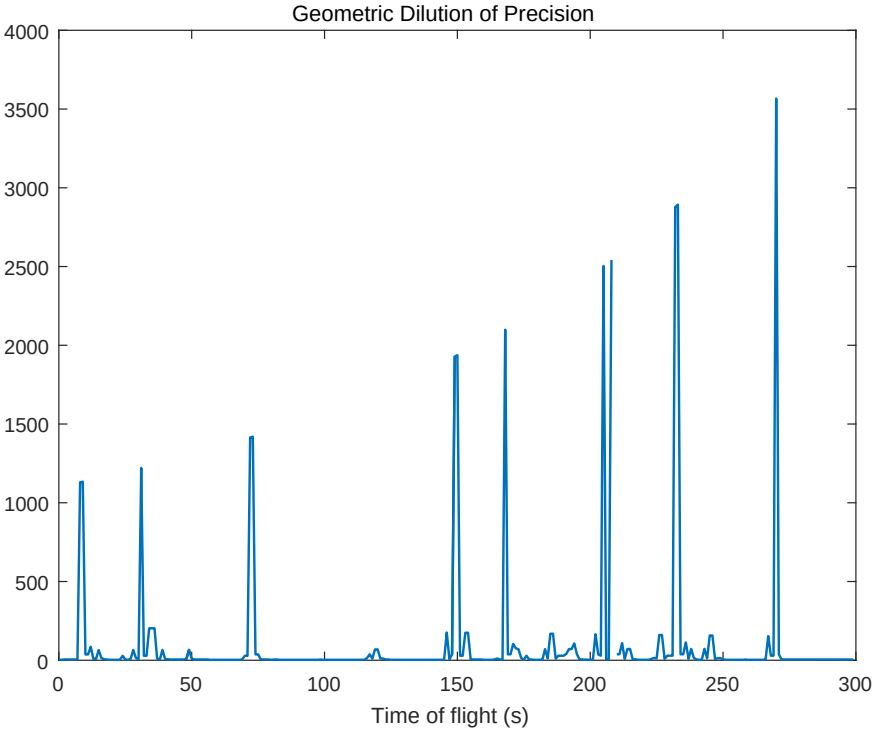

Figure 4.8: Geometric Dilution of Precision for all time of Flight 1

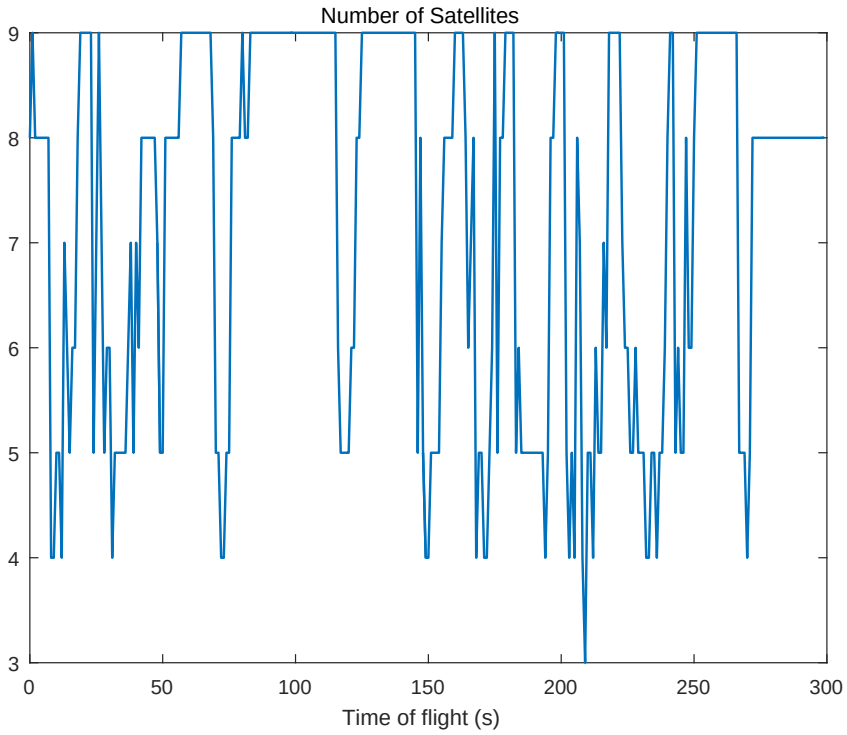

Figure 4.9: Number of Satellites observed of Flight 1

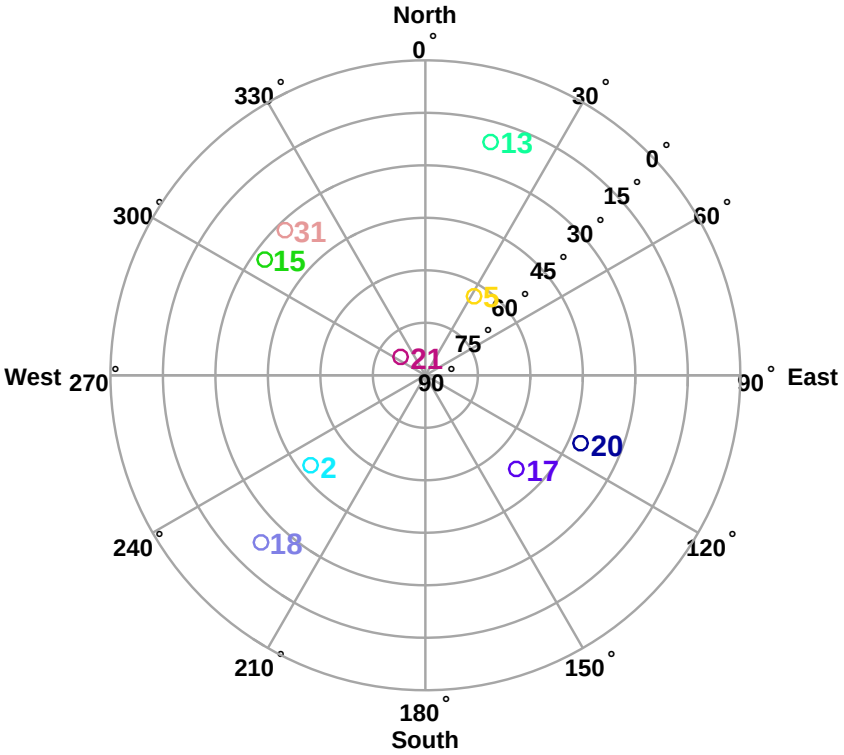

Figure 4.10: Best GDOP of Flight 1 = 2.747

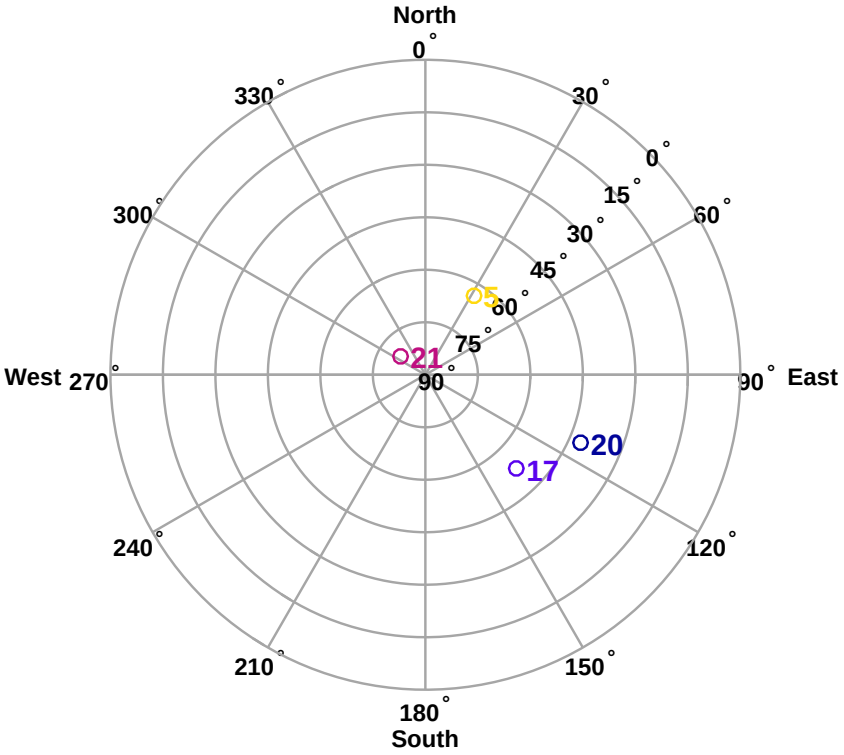

Figure 4.11: Worst GOP of Flight 1 = 3567

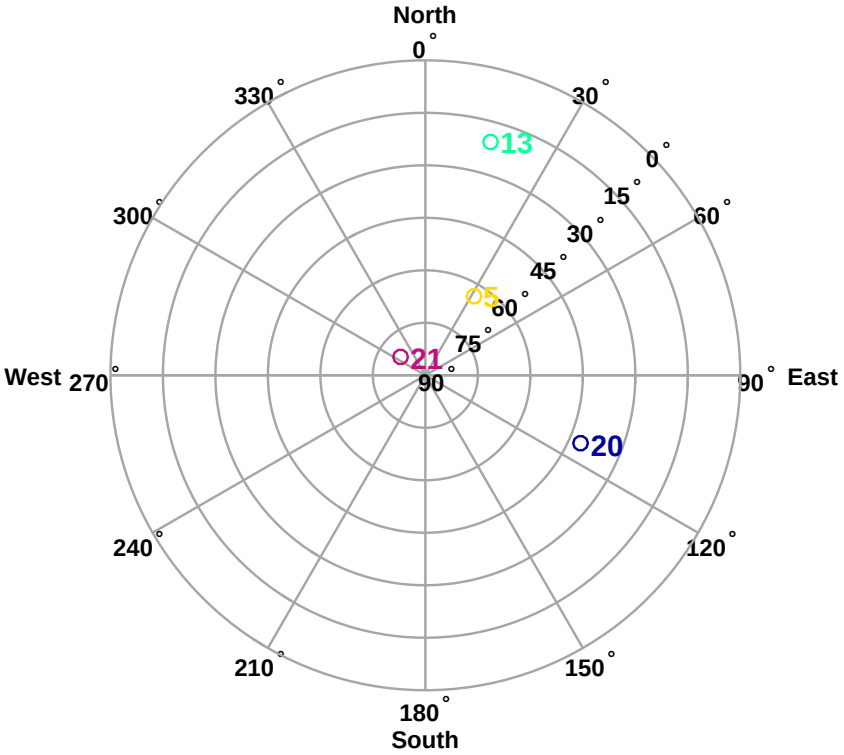

Figure 4.12: Best GOP with 4 satellites of Flight 1 = 36.96

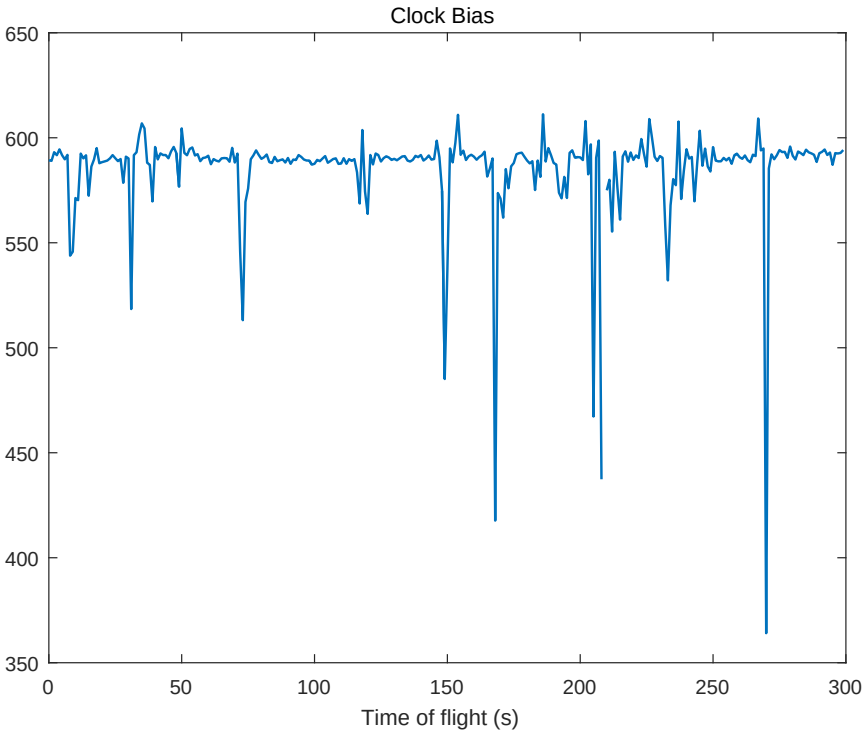

Figure 4.13: Clock Bias of Flight 1

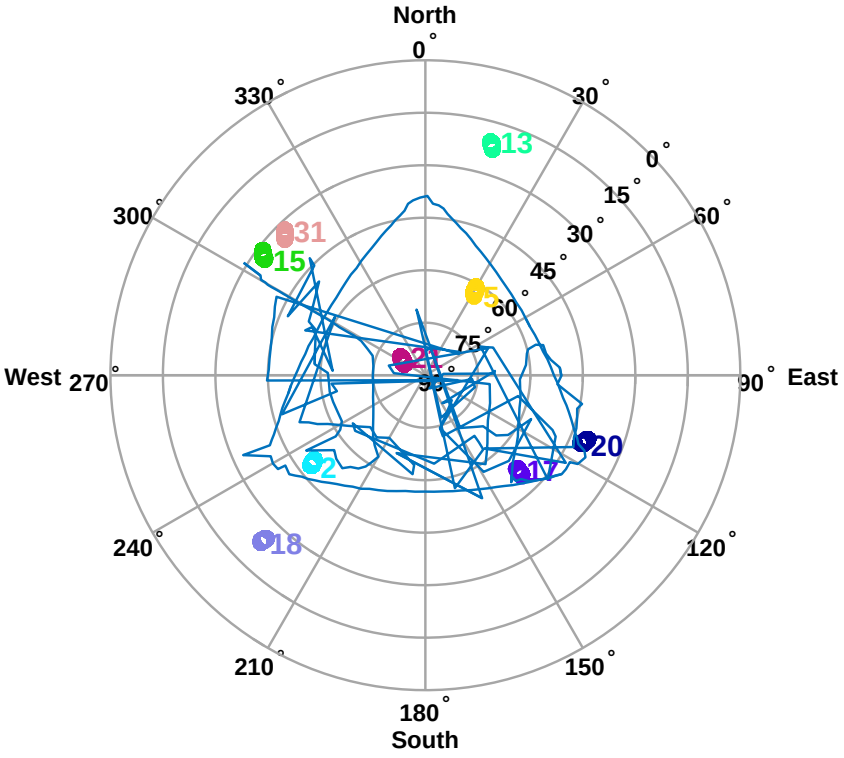

Figure 4.14: UAV Flight 2 polar trace of azimuth and elevation and location of observed satellites from ground station at [Lat 34.76°,Long: 150.03°E, Alt: 680m]

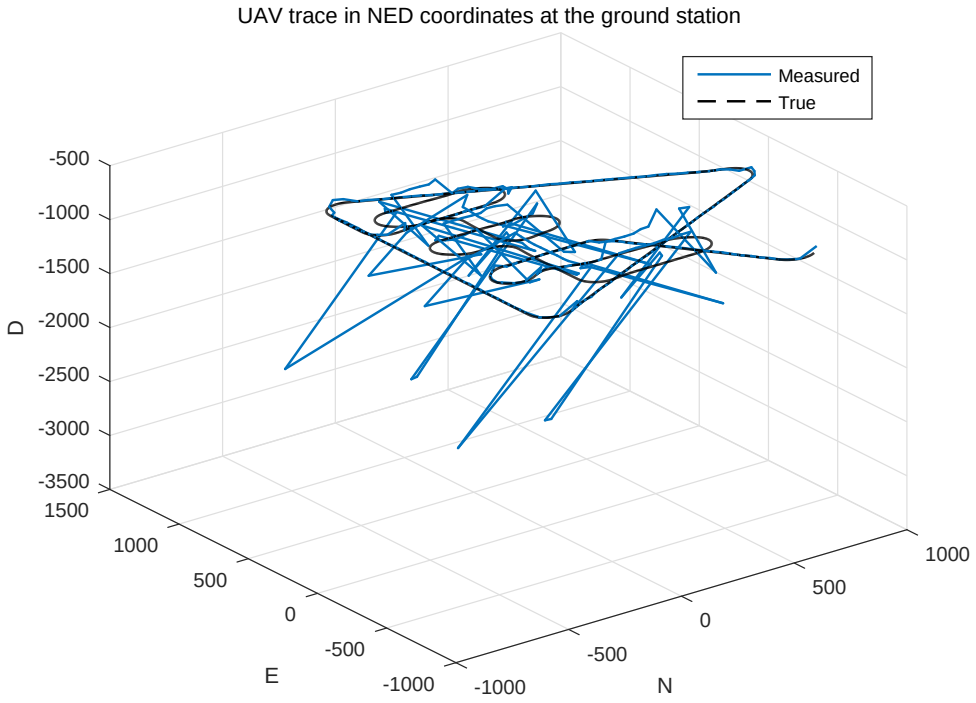

Figure 4.15: UAV Flight 2 trace in NED coordinates from the ground station at [Lat 34.76°,Long: 150.03°E, Alt: 680m]

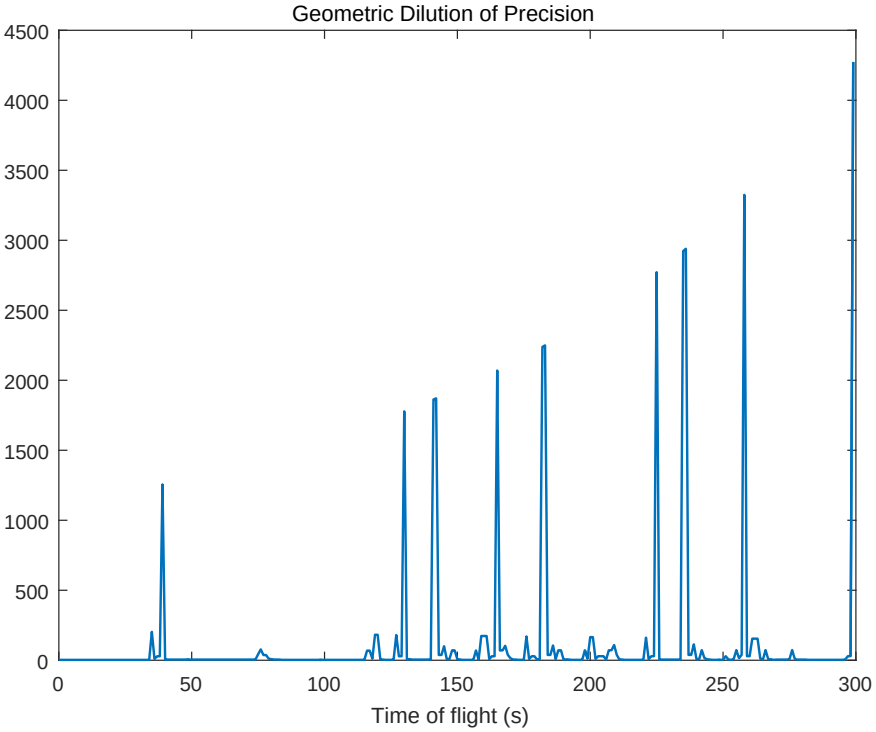

Figure 4.16: Geometric DOP for all time Flight 2

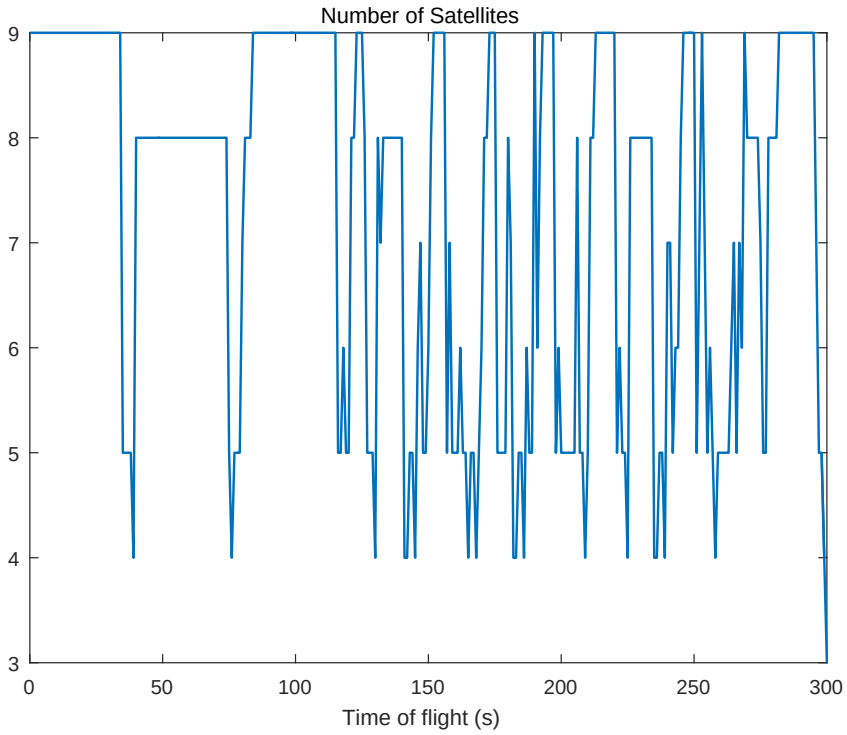

Figure 4.17: Number of satellites observed Flight 2

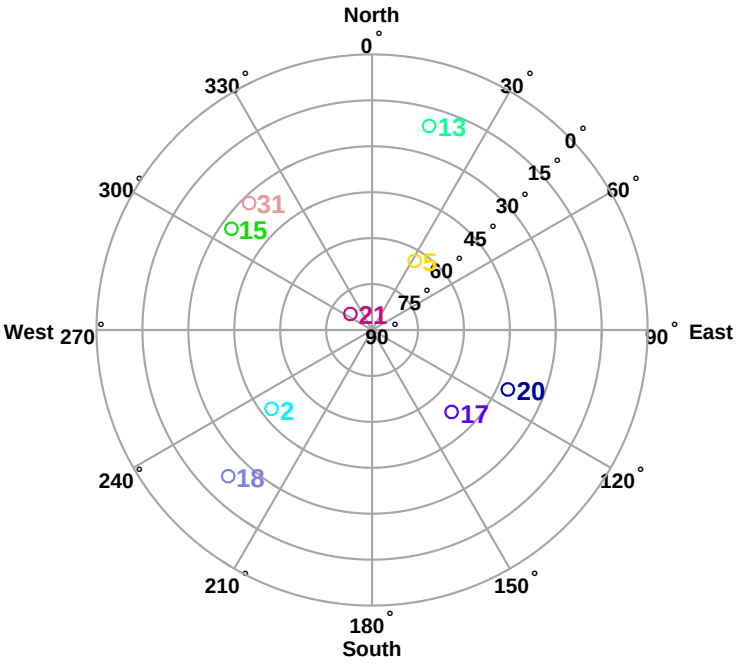

Figure 4.18: Best GDOP of Flight 2 = 2.74

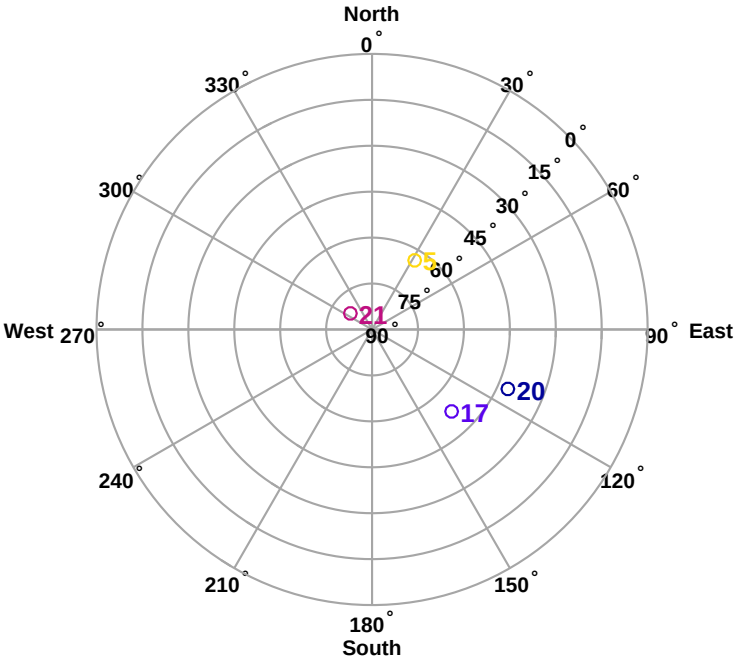

Figure 4.19: Worst GDOP of Flight 2 = 4274

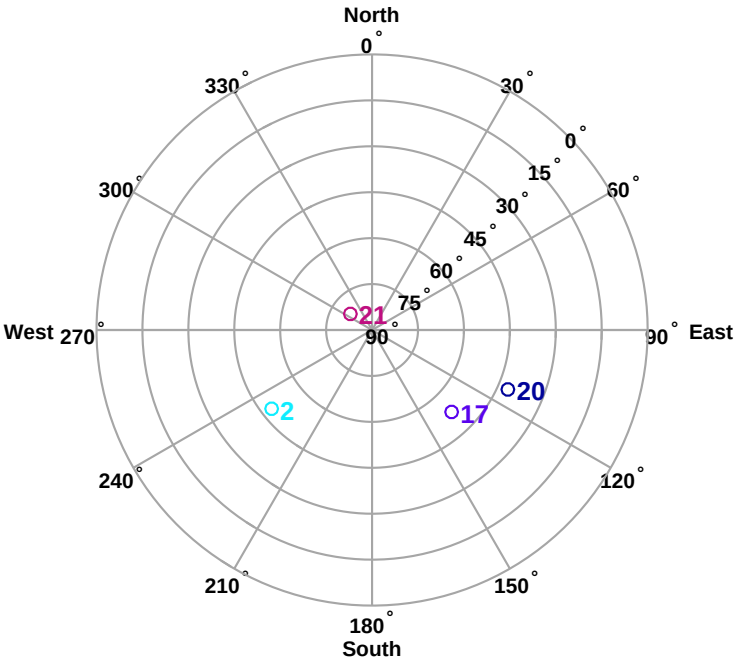

Figure 4.20: Best GDOP with four satellites of Flight 2 = 77.5

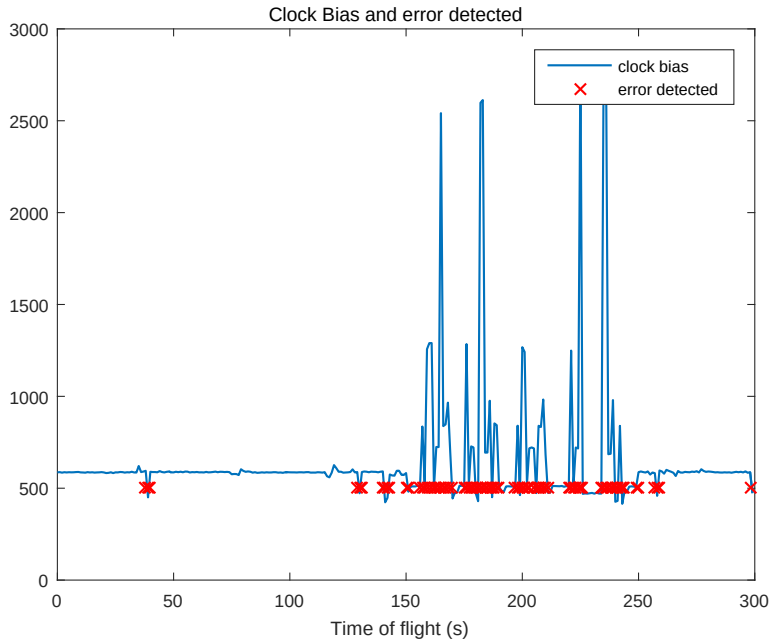

Figure 4.21: Clock Bias of Flight 2 with detection of errors

5. Appendix B: Question 2

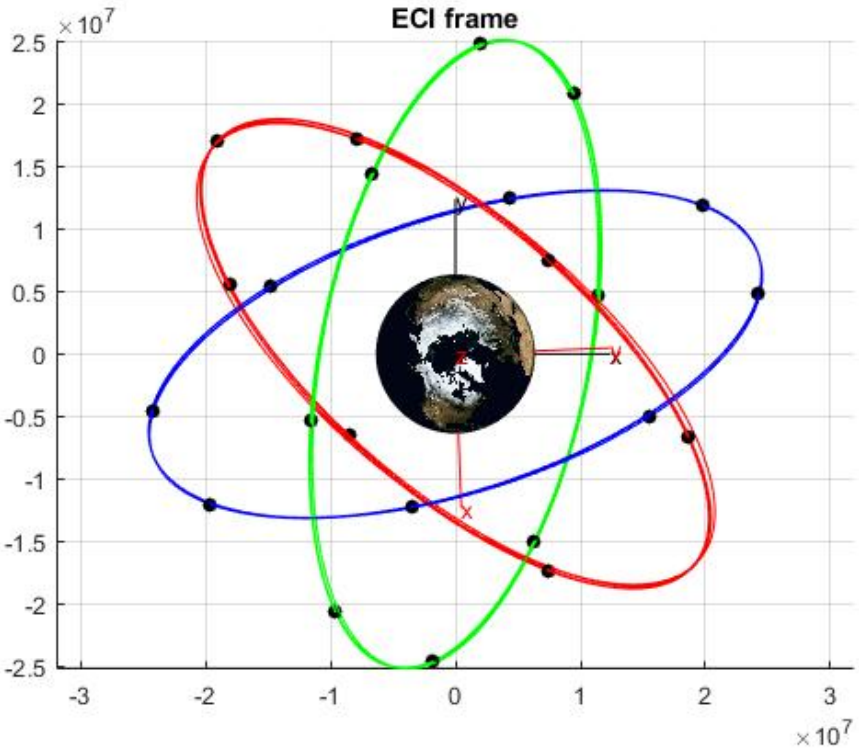

Figure 5.1

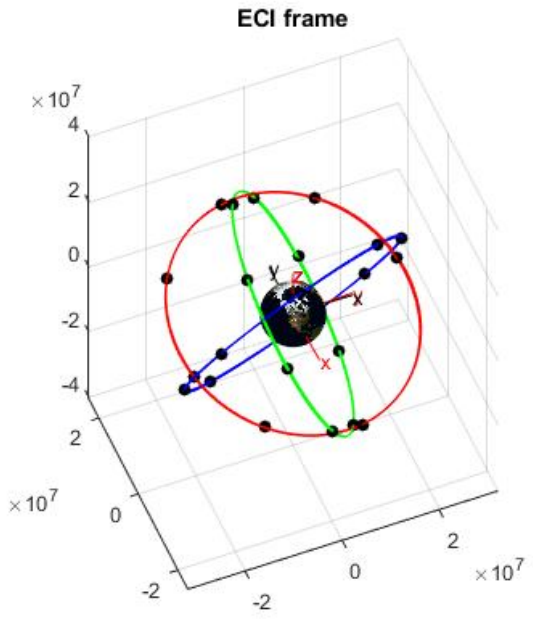

Figure 5.2

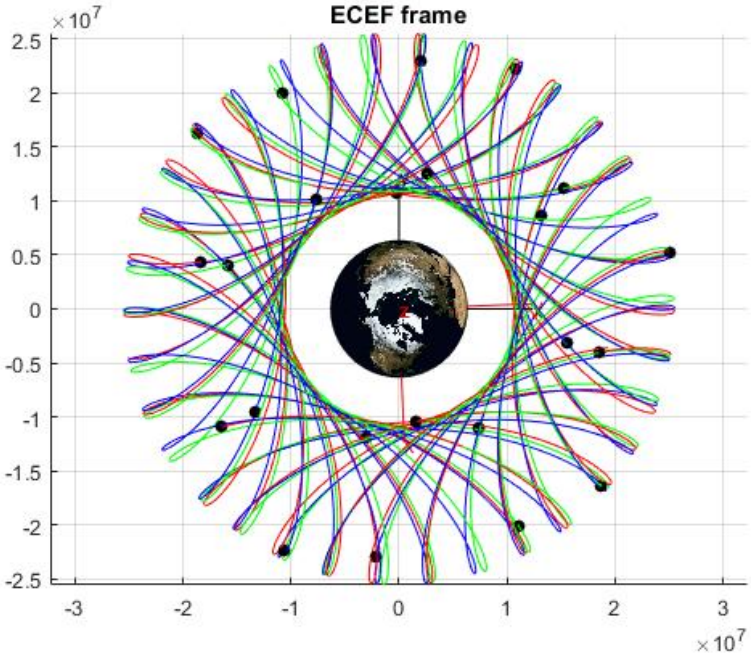

Figure 5.3

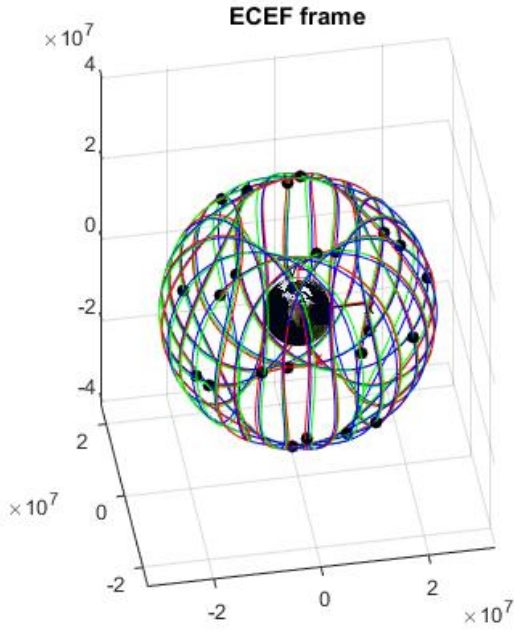

Figure 5.4

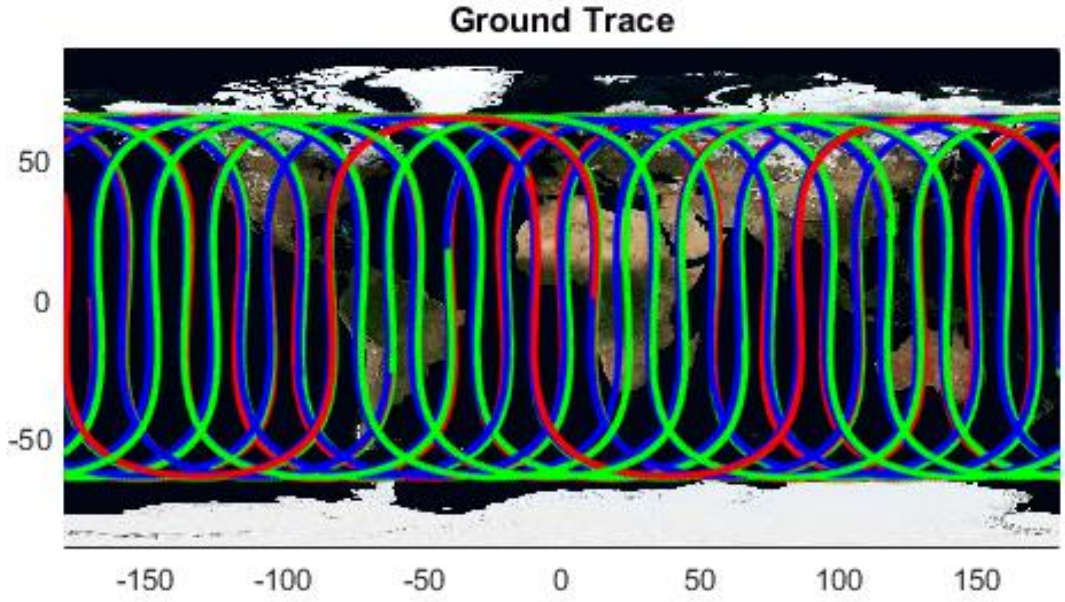

Figure 5.5

Figure 5.6: text

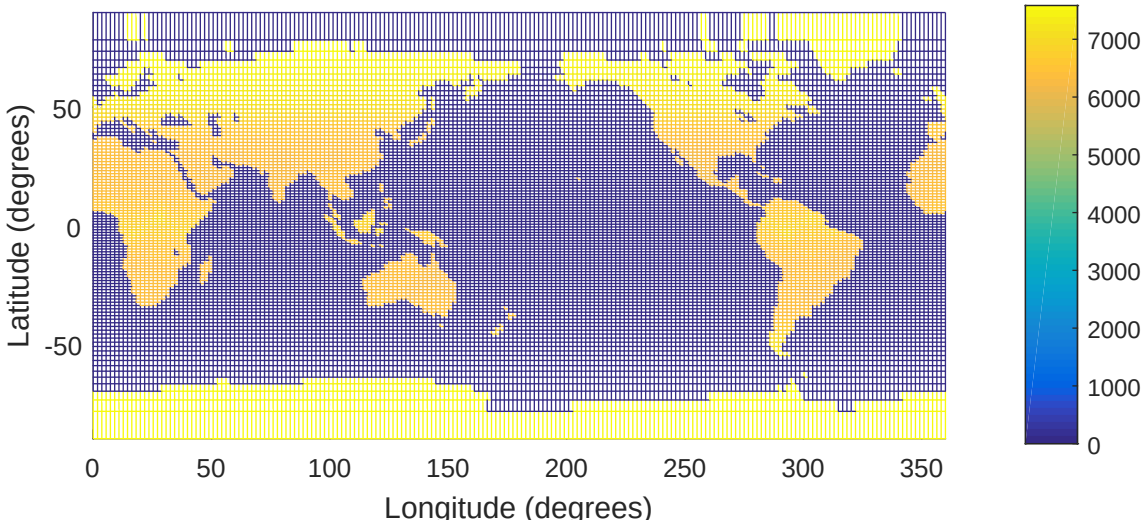

Figure 5.7: text

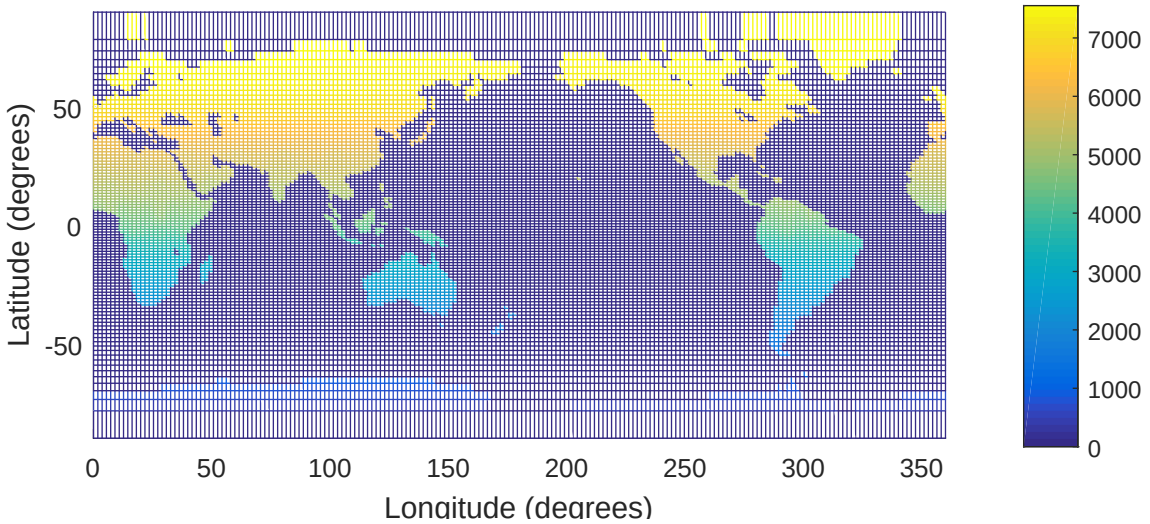

Figure 5.8: text

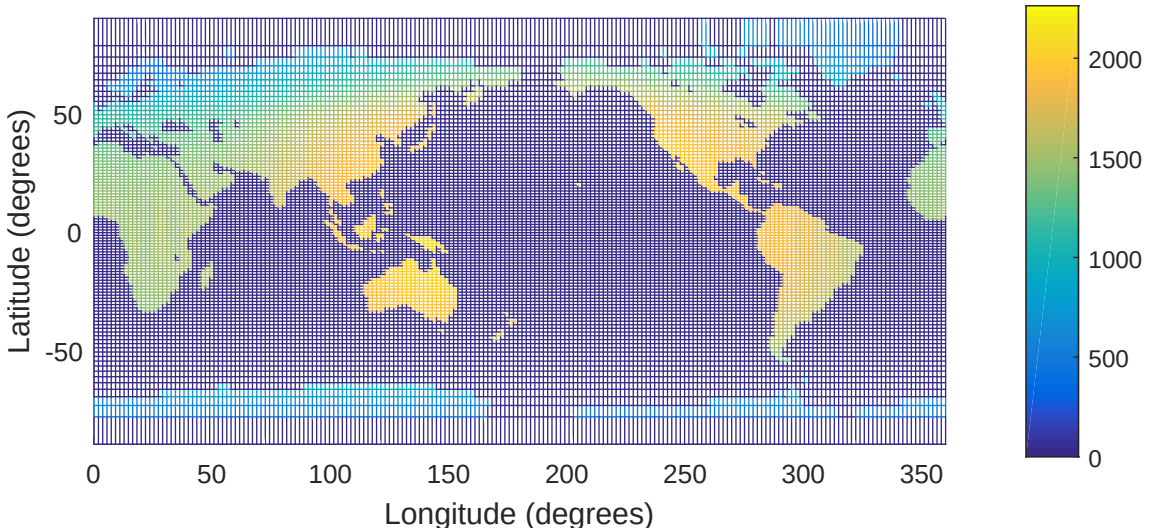

Figure 5.9: text

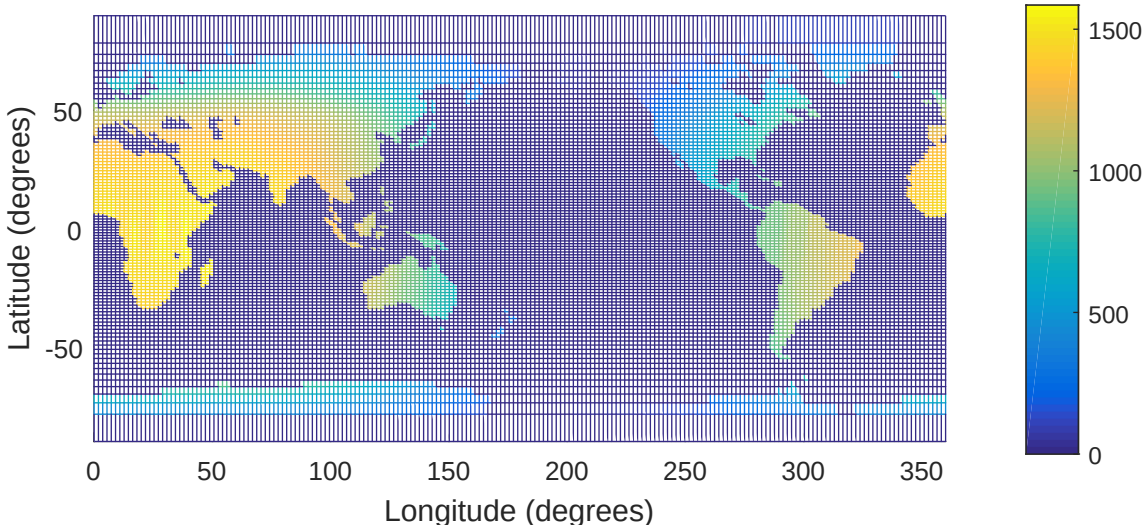

Figure 5.10: text

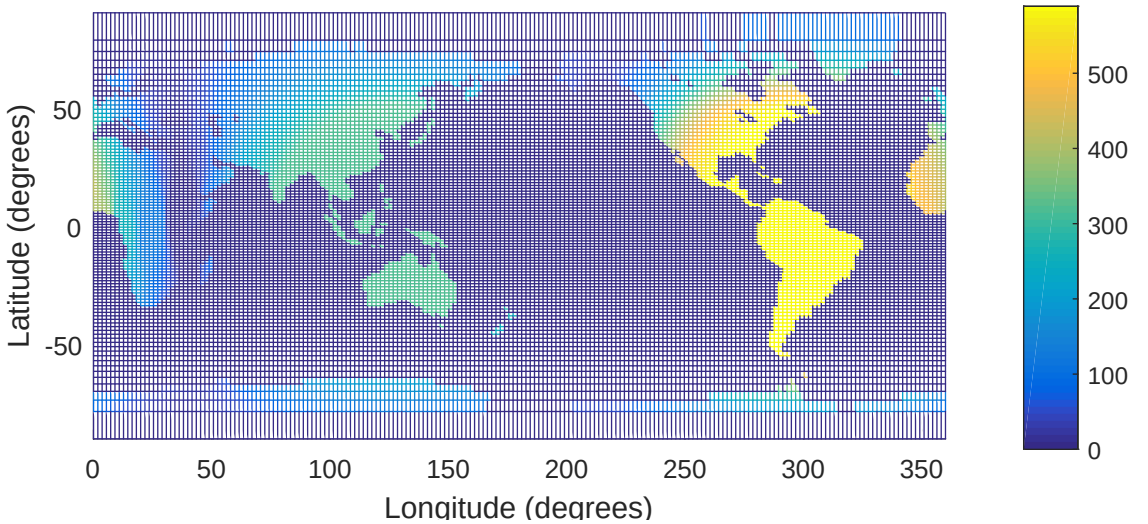

Figure 5.11: text

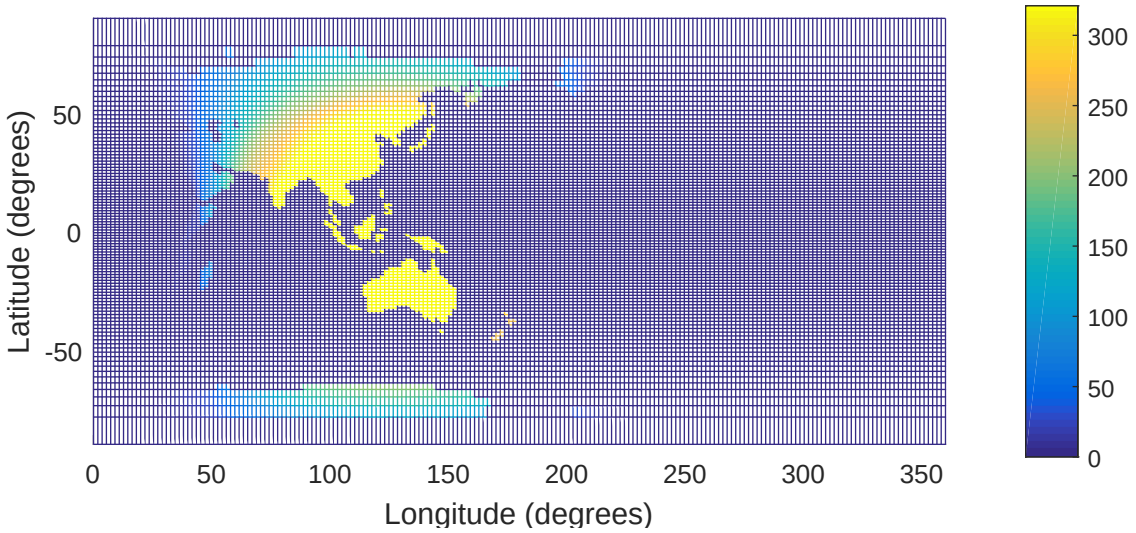

Figure 5.12: text